Neuropsychologia 163 (2021) 108068

Contents lists available at ScienceDirect

Neuropsychologia

journal homepage: www.elsevier.com/locate/neuropsychologia

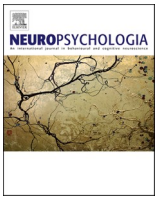

Inhibition of return in time-lapse: Brain Rhythms during grip force control for spatial attention

Filippo Zappasodi [a,b], Pierpaolo Croce [a], Rosalia Di Matteo [a], Marcella Brunetti [a,b,*]

[a] Department of Neuroscience, Imaging and Clinical Sciences, 'Gabriele d'Annunzio' University, Chieti, Italy
[b] Institute for Advanced Biomedical Technologies, 'Gabriele d'Annunzio' University, Chieti, Italy

A B S T R A C T

The inhibition of return (IoR) is the observable slowed response to a target at a cued position for cue-target intervals of longer than 300 ms; when there has been enough time to disengage from a previously-cued location, an inhibitory after-effect can be observed. Studies aimed at understanding whether mechanisms underlying IoR act at a perceptual/attentional or a later response-execution stage have offered divergent results. Though focusing on the brain's responses to cue-target intervals can offer significant information on the nature of IoR, few studies have investigated neural activity during this interval; these studies suggest the generation of inhibitory tags on the spatial coordinates of the previously attended position which, in turn, inhibit motor programming toward that position. As such, a cue-target task was administered in this study; the rhythmic activity of EEG signals on the entire cue-target interval was measured to determine whether IoR is referred to early or late response processing stages. A visually-guided force variation during isometric contraction, instead of a key press response, was required to reduce the effect of motor response initiation. Our results indicated the prominent involvement of the fronto-parietal and occipital cortical areas post-cue appearance, with a peculiar theta band modulation characterizing the posterior parietal cortex. Theta activity in this region was enhanced post-cue onset, decreased over time, and was enhanced again when a target appeared in an unexpected location rather than in a cued position. This suggests that the mechanism that generates IoR sequentially affects perceptual/attentional processing and motor preparation rather than response execution.

1. Introduction

Inhibition of return (IoR) is the slowed response to a target at a previously inspected location in conditions with a stimulus onset asynchrony (SOA) of longer than 300 ms. Traditionally, IoR has been considered a phenomenon based on the capturing of attention by a cue in a peripheral position and the subsequent inhibition of returning attention to that position once it had been withdrawn from it (Posner et al., 1985). Specifically, after a peripheral location has been explored, the facilitation of sensory processing can be expected for subsequent stimuli in that location. Even so, when attention has had enough time to disengage from that location (i.e., in cases of a long SOA), an inhibitory after-effect can be observed (Klein, 2000). The stability of the IoR effect has been proven for SOAs ranging from 300 to 1600 ms and its strength has been verified until 3 s after the onset of the cue (Samuel and Kat, 2003).

The debate on this topic has mainly centred on whether IoR depends on a mechanism that acts at a perceptual/attentional stage of processing or one that acts at a later response stage, essentially whether IoR is generated by a capture of attention to the cued location or by the activation of an oculomotor program toward the cued location, even in the absence of eye movements. The first key work on this topic was that of Rafal et al., who demonstrated that the IoR effect can be caused by the activation of the oculomotor system (Rafal et al., 1989). Additionally, Klein and Taylor offered a motor bias hypothesis by defining IoR as a "reluctance" to respond to a stimulus coming from an inhibited location (Klein and Taylor, 1994). Chica et al. demonstrated that the key mechanism of motor IoR, which is generated by eye movements toward the cue and/or the target, did not have behavioural effects on perceptual processing but did have these effects on both motor preparation and response decision processes (Chica et al., 2010). Furthermore, according to Prime and Ward (2004), when eye movements were prevented, the IoR effect was to be referred to the decisional and premotor stages but not to the motor ones. Conversely, Berlucchi argued that the mechanism underlying IoR involves primarily sensorial, rather than attentional, components (Berlucchi, 2006).

The electroencephalographic (EEG) technique has often been used to examine the temporal dynamics of the brain activity that accompanies a cue target task in order to clarify the nature of IoR. The negative differences between event related potential (ERP) components due to either valid or invalid cue targets are thought to be due to a reduction in the efficiency of valid cue target processing. Specifically, delayed target-

* Corresponding author. University 'G. d'Annunzio' of Chieti-Pescara, Institute for Advanced Biomedical Technologies, Via Luigi Polacchi 13, Chieti, 66100, Italy.
E-mail address: marcella.brunetti@unich.it (M. Brunetti).

https://doi.org/10.1016/j.neuropsychologia.2021.108068
Received 13 May 2021; Received in revised form 15 September 2021; Accepted 18 October 2021
Available online 20 October 2021

locked latencies of lateralized readiness potentials have been observed when comparing valid cue targets with invalid ones, suggesting IoR's association with pre-motor processes rather than with the inhibition of motor processes (Prime and Ward, 2004, 2006). Based on these findings, and drawing inspiration from a previous model, the authors proposed that IoR is responsible for the reduction in the salience of the cued location. Consequently, the processing of a salient target could be faster in cases of non-cued locations, for which negative salience does not need to be overcome, than in cases of cued ones. This reduction in target processing efficacy for cued positions may explain the subsequent increase in response times (Prime and Ward, 2006). P1 and N2pc, two components that reflect covert attention deployment, have been used to assess the effects of IoR on both perceptual processing (McDonald and Ward, 1999) and attentional deployment (McDonald et al., 2009); results have indicated a reduced P1 for cued targets. Furthermore, the authors concluded that the inhibition mechanism at the foundation of IoR acts by reducing the probability of shifting attention to attended locations rather than delaying the covert deployment of attention itself.

Focusing on the brain's responses to cues can be highly informative regarding the nature of IoR, though few studies have investigated neural activity during the cue target interval. Tian et al. (2011) developed a theoretical model of IoR, identifying the areas that are activated at different stages post-cue onset. Focusing on the cue stimulates early visual areas, including the superior colliculus, which then sends signals to cortical regions (specifically the parietal areas and frontal eye field regions), thus creating inhibitory tags on the coordinates derived from the spatial properties of the cue and inhibiting subsequent eye movements to that location (i.e., IoR).

The neural bases of IoR have been also studied via the observation of the amplitude modulation of EEG oscillatory activity following cue/target stimuli. Pastötter et al. (2008), for example, examined changes in event-related desynchronization/synchronization (ERD/ERS) patterns in cases of two IoR designs, namely target–target and cue-target. They found an increased contralateral beta (15–25 Hz) ERS in the target–target design and a decreased beta ERD in the cue-target design; they then inferred that IoR emerges from the inhibition of motor processes, which affect different mechanisms depending on the utilized design. Another recent study demonstrated that IoR affects response-related oscillatory EEG activity, and hypothesized that an attention-driven reduction in somato-motor processing occurres prior to the response to previously cued target locations (Amenedo et al., 2015).

When examining the literature, the most common tasks used to study the temporal dynamics of IoR required motor responses based on a key press. This procedure entails an off-on transition from no motor action to a voluntary motor action. In other words, in a typical detection task, participants are required to detect the target and then rapidly press a button. During this process, however, the IoR effect observed on reaction times could be due to slowed orienting of attention, slowed sensorial/perceptual processing, and/or slowed initiation of the motor response (see Chica et al., 2010).

Accordingly, we attempted to reduce the effects of motor response initiation by administering a task in which a force variation during a grip control task was required in place of a key press response. Participants, based on task conditions, were asked to precisely control, and online adjust using the visual feedback, the isometric grip force applied to a tool (i.e. a bulb pump) held between their thumb and the palm of the hand. The ability to scaling of finger force during object manipulation represents a motor command controlled by specific regions (Kuhtz-Buschbeck et al., 2001). Especially, the critical role of posterior parietal cortex in the hand shaping and grip force scaling needed to adequately perform a skilled hand movement has been observed by means different techniques (Davare et al., 2007; Zaepffel and Brochier, 2012). Differently from a typical key press task, in which hand motor activation starts whit target onset, here the hand muscular contraction started before cue appearance. In a departure from typical IoR tasks, our participants did not have to plan a motor program from scratch in the cue-target period; they instead needed to be ready to adjust their applied force. This "continuous" motor control (as opposed to an off-on action) during the entire cue-target.

To our knowledge, this is the first study in which the dynamics of the IoR effect have been studied by means of a visuomotor isometric contraction task. Previous studies investigated patterns of coupling in the cortical areas during visuomotor integration tasks, highlighting that visual and proprioceptive sensory inputs must be integrated with motor control signals through the mediation of fronto-parietal networks (see (Schnitzler and Gross, 2005)). Specifically, EEG studies have shown decreases in alpha and lower beta power in the central, parietal, and occipital brain areas (Classen et al., 1998). More recently, Papadelis et al. studied this topic by means of magnetoencephalography and a visuomotor task that was designed to continuously require visual sensory feedback in order to control the exerted force by means of a pinch motor command (Papadelis et al., 2016); they subsequently identified a network that is active during visuo-motor integration and includes primary sensory areas, the contralateral primary motor cortex, and secondary integration areas.

Here, we have adapted this kind of visuomotor isometric contraction task to the study of visuo-spatial attention. Our purpose was to determine the temporal dynamics of IoR from the cue onset until the target appearance. To reduce motor interference, our participants initiated contraction prior to cue appearance, maintained a constant contraction level throughout the cue-target interval, and changed the applied force level in response to the target. Analysis of the brain's rhythm during the cue-target interval could offer significant insight regarding the information processing stage that is the foundation of IoR, especially considering the lower frequency bands. Indeed, in the mammalian brain, oscillatory networks in the lower frequency bands (<12 Hz) like the theta band (4–8 Hz) are often thought to be a key mechanism for brain-wide interaction between distal regions (von Stein et al., 2000). In particular, increased rhythmic activity of the theta band in the frontal cortex is a sign of improved task performance and sustained attention that reflects the level of cognitive attention required by the given task (Cavanagh and Frank, 2004; Clayton et al., 2015). In addition, theta oscillations in frontal areas have been known to form a phase-coherent network with task-related brain regions, including sensory cortices (Benchenane et al., 2011; Liebe et al., 2012). The emergence of a theta oscillation network indicates active neuronal processing for cognitive functions like sustained attention (Clayton et al., 2015), cognitive control (Cavanagh and Frank, 2004), and working memory (Sauseng et al., 2010). Another frequency band traditionally observed during visuo-motor tasks is the beta (15–30 Hz) band; the amplitude of this rhythm has been shown to be modulated both during and after the preparation and performance of produced or observed movements (Pfurtscheller et al., 1996a, 1996b; Brunetti et al., 2014). To this end, thalamocortical coherence during movement preparation, isometric contraction, and at rest were also observed in the beta band (see Schnitzler and Gross, 2005).

After reviewing the literature on visuomotor tasks, we hypothesized that we would observe different modulations of the theta and beta rhythms during invalid and valid target processing. Specifically, the amplitude of the middle frontal theta was expected to be enhanced in the invalid condition, during which the applied force level should be rapidly adjusted according to visual feedback. Conversely, we expected that an inhibitory process reduces readiness, and therefore theta amplitude, for a target appearing in the cued position (i.e., during the valid condition). Finally, we aimed to clarify whether IoR was generated by a mechanism acting during an early attentional/premotor stage or a later motor one by integrating temporal information and source localization of oscillation activity.

2. Methods

2.1. Participants

Eighteen healthy subjects (six female, mean age of 21.3 ± 1.8 years) were recruited for the study. All subjects were right-handed as assessed by the Edinburgh Handedness Inventory (mean and standard deviation: 71 ± 20 (Oldfield, 1971),), reported no history of neurological or psychiatric disease, and were not taking psychoactive medications at the time of the study. The experimental protocol was approved by the local ethics board of the University G.D'annunzio, and all subjects signed an informed consent form.

2.2. Experimental task

Subjects participated in a cue-target task that required the continuous adjustment of the steady-state isometric contraction of the fingers according to visual feedback on a screen. Specifically, they had to move a cursor toward prompted positions in the vertical plane by continuously adjusting the isometric contraction force with which they pressed their thumb against a bulb pump held in the palm of their hand (Fig. 1); once they reached the requested position, they had to maintain a stable finger contraction. A sensor inside the bulb was able to transduce the pressure and display the level of exerted force in the form of a black horizontal bar moving up and down on a green vertical bar. The requested contraction level (the desired vertical position) was indicated by two dashes on the sides of the green vertical bar (Fig. 1). The goal positions on the vertical green bar corresponded to 5%, 10%, 15%, 20%, and 25% of the individual's maximal voluntary contraction (MVC). This value was acquired at the beginning of the experimental session by measuring three repetitions of contractions maintained for 1 s each and was used to determine the force each subject needed to exert to reach different positions on the green bar. The value of 15% of the individual's MVC corresponded to the force they needed to exert to keep the black horizontal bar halfway up the green vertical bar. The values of 5% and 10% of MVC corresponded to the force they needed to exert to reach two different points below the middle of the green vertical bar, requiring a decrease in the contraction, while the values of 20% and 25% of MVC corresponded to the force they needed to exert to reach two different points above the middle of the green vertical bar, requiring an increase in the contraction.

The experimental task consisted of 192 16-s trials; each trial was made up as follows (Fig. 1):

Rest period (6 s): Trials began with a 6 s rest period; the participant kept their eyes open.

Contraction period (4 s): At the appearance of two horizontal dashes (start dashes) on either side of the green vertical bar (at mid-height, corresponding to 15% MVC), subjects were asked to raise the black horizonal bar to this level and maintain it for 4 s by adjusting their exerted force.

Cue period (2 s): A cue consisting of an additional pair of horizontal dashes (cue dashes) was then presented at a different height on the green vertical bar; this cue corresponded to one of the aforementioned positions (5%, 10%, 20%, or 25% of MVC). Subjects were informed that the new pair of dashes potentially, though not necessarily, represented their next target. They were asked to maintain the exerted force (i.e., the position of the black bar) until the mid-height dashes (i.e., the start dashes) disappeared; this disappearance acted as a go signal. In this way, their gaze remained in the central position during the entire cue period.

Target period (4 s): A new pair of dashes (target dashes) then appeared at one of the five aforementioned positions (5%, 10%, 15%, 20%, or 25% of MVC), and subjects were instructed to reach the new target level as quickly as possible by adjusting their contraction and maintaining it for 4 s. Three different experimental conditions could randomly be presented (Fig. 1, right):

- VALID_GO: Target dashes appeared in the same position as the cue dashes.
- INVALID_GO: Target dashes appeared in a different position than the cue dashes.
- INVALID_NO GO: Target dashes appeared at mid-height, meaning that subjects had to maintain their contraction to keep the bar still.

To control for effects related to the attending to a position, a NEUTRAL condition was also included in the experimental trials (Fig. 1, left). In the control trial, a pair of target-dashes were delivered immediately after the contraction period and subjects were asked to reach that target level as quickly as possible and maintain the contraction for 4 s. Thus, each NEUTRAL trial was made up of rest, contraction, and target periods; no cue dashes were delivered.

Forty-eight trials were acquired for each condition. To avoid fatiguing effects, the sequence of trials was split into four blocks of 48 trials each: three blocks randomly including VALID_GO, INVALID_GO, and INVALID_NO GO trials, and one block including NEUTRAL trials. Pauses were intermingled between blocks, that were randomly presented across subjects. Before the experimental trials began, each

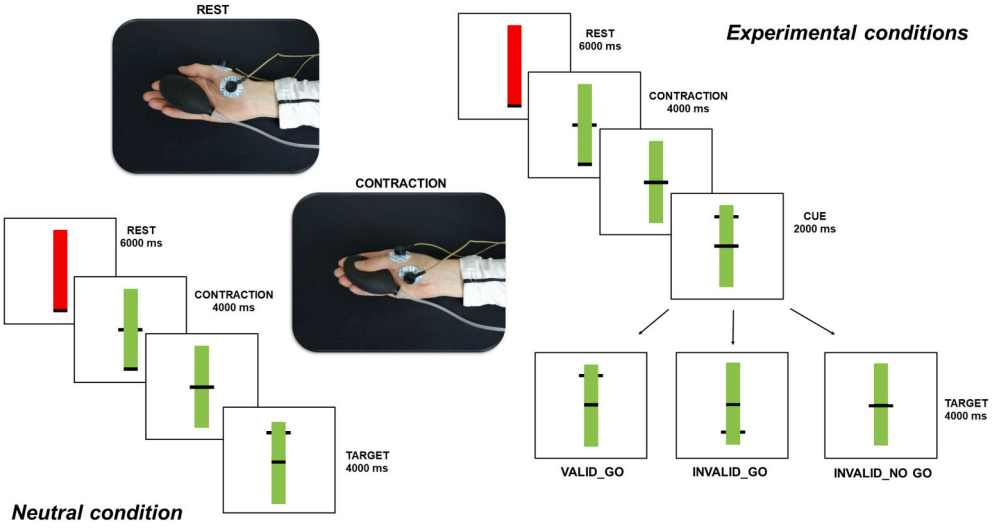

Fig. 1. Representation of the three conditions used in experimental trials and the neutral condition. Movement during the steady state contraction is shown, subject pressed a bulb by moving the thumb of the right hand against the other fingers. Periods of movement were intermingled with periods of rest.

subject trained for 5 min in order to make him\her comfortable with the task. This time was enough for the subject to reach a stable performance plateau. Three minutes of EEG data at rest with eyes closed and 3 min of EEG data at rest with eyes open were also acquired prior to task execution. In sum, each experimental session was about 1 h long.

2.3. EEG recording

Electric activity in the brain was recorded using a 128-channel EEG system (Electrical Geodesic Inc, EEG System Net 300). Electromyographic (EMG) activity in the right Opponens Pollicis Brevis and the time-course of the exerted force by the home-made pressure sensor were measured simultaneously. Given the high variability of EMG in estimating time performance during force variation, EMG data were not considered for further analysis, in line with previous literature using force level to estimate performance (Davare et al., 2007).

Skin/electrode impedance was measured before each EEG recording and kept below 50 kΩ. EEG data was sampled at 1000 Hz and processed offline. The position of each electrode and of four anatomical landmarks (preauricular points, nasion, vertex) were acquired by means of a 3D digitizer (Polhemus, 3Space Fastrak) at the end of the experimental session to allow for the definition of a subject head-based coordinate system.

2.4. Behavioural data analysis

To evaluate the stability of the exerted force during a given time interval, the relative standard deviation with respect to the target force value was considered. Specifically, if $x_1, x_2, \ldots x_N$ were the N samples of the force during the time interval and RFL was the required force level, then the Force Variation index (FVi) could be calculated as:

$$FVi = \sqrt{\frac{1}{N}\sum_{i}^{N}(x_i - RFL)^2}$$

The more stable the contraction, the lower the FVi value. A FVi of zero corresponds to a level of the contraction equal to the RFL over time, i.e., maximal stability and optimal performance.

The temporal dynamics of the force exerted during each trial was obtained for each subject. In particular, time to movement (TtM) was calculated as the time needed to reach either 90% or 110% of the new level, i.e., from the instant of the change in force on the screen until the time at which the force level has reached 90% (when the amount of force has increased) or 110% (when the amount of force has decreased) of the new level (Fig. 2A). For each trial, two TtMs were calculated, one at the beginning of the movement (TtM_1), representing the time needed to switch between rest and movement to 15% MVC (starting level), and the other at the beginning of the target period upon presentation of the new target level (TtM_2), representing the time needed to switch from 15% MVC to the indicated target level (5%, 10%, 20%, or 25% MVC). Mean values across trials were obtained for each subject. Averaged TtM_2 was calculated separately for the VALID_GO, INVALID_GO, and NEUTRAL conditions. Six time intervals were identified for subsequent analysis (Fig. 2A): the pre_C interval corresponded to 1 s before cue onset, C1 and C2 were two consecutive intervals of the same duration (1 s) defined from the cue onset to target onset, and T1, T2, and T3 were three intervals of 1, 1.5, and 1.5 s, respectively, from target onset to the end of the trial. Fig. 2B shows the overall average of the exerted force in all experimental conditions across all subjects and trials.

2.5. EEG data analysis

For each subject, the EEG time course was visually inspected to

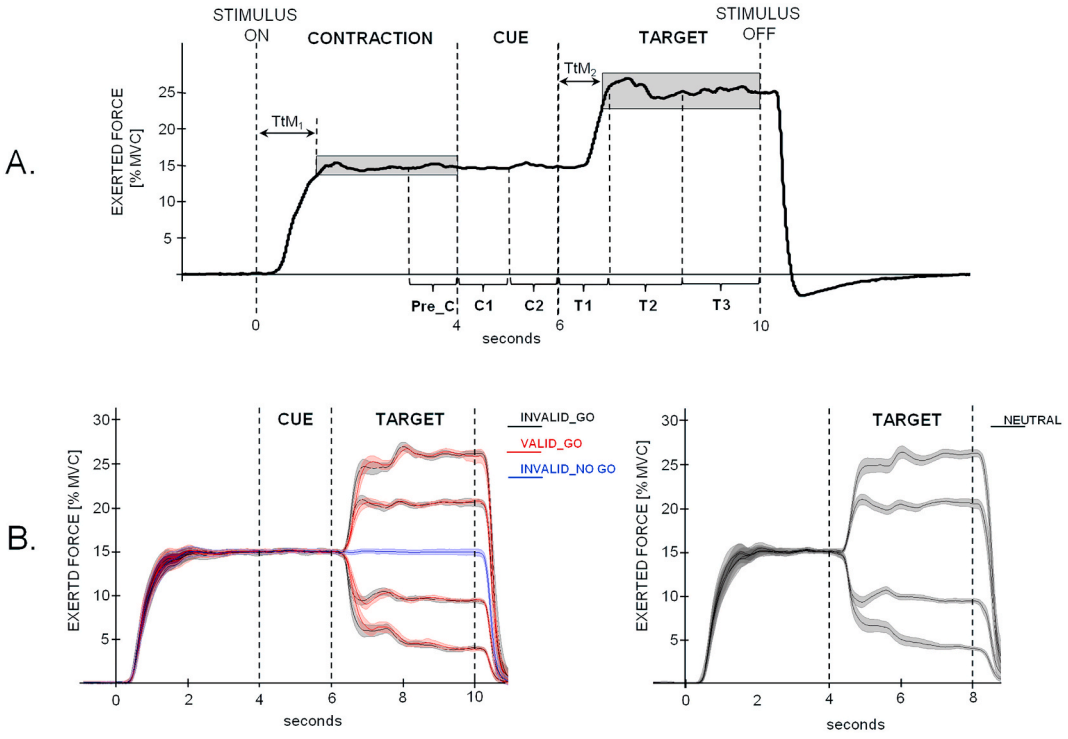

Fig. 2. A. Example of exerted force (expressed as percentage of Maximal Voluntary Contraction, MVC) during a trial. The times to reach the requested level of force (TtM1 and TtM2) and the time intervals used for the analysis are shown (Pre_C, C1, C2, T1, …). Gray boxes indicate the 90%–110% interval of the requested level (15% in the contraction period and 25% in the target period in this trial). **B.** Grand average of the force level among all the trials for all the four experimental conditions (on the left: INVALID_GO: black, VALID_GO: red; INVALID_NO GO: blue; on the right: NEUTRAL) and all the requested level in the task period (5%, 10%, 20%, 25% for INVALID_GO, VALID_GO and NEUTRAL and 15% for the INVALID_NO GO). Mean values and standard error of the mean are shown. . (For interpretation of the references to colour in this figure legend, the reader is referred to the Web version of this article.)

remove particularly noisy channels or recording segments that were highly contaminated by movement artefacts. Data was then filtered between 1 and 80 Hz and notch filtered at 50 Hz (Butterworth filter of 2nd order, forward and back filtering). A semiautomatic procedure based on Independent Component Analysis (ICA) was then applied to remove ocular and cardiac artefacts (Barbati et al., 2004; Croce et al., 2019).

EEG analysis was partially done using FieldTrip software (Oostenveld et al., 2011). Time–frequency representations (TFRs) were estimated in 16 s time windows starting 3 s prior to the presentation of the movement onset. Specifically, TFRs for each EEG channel were calculated between 2 and 45 Hz, with a frequency resolution of 1 Hz, using the multitaper method (Mitra and Pesaran, 1999). The estimate was carried out separately for each of the three conditions (VALID_GO, INVALID_GO, INVALID_NO GO) and for the control condition (NEUTRAL). Accordingly, the time course of power modulation was evaluated for each frequency by calculating the relative changes in the TFR of power after the presentation of movement onset (Pow) with respect to the mean power during a baseline period of 2 s prior to onset (Pow_{Bas}). To this end, Event-Related Synchronization (ERS) or Event-Related Desynchronization (ERD) (Neuper and Pfurtscheller, 2001; Pfurtscheller and Lopes da Silva, 1999) values were obtained using:

$$ERD/ERS = 100(Pow - Pow_{Bas})/Pow_{Bas}$$

The whole-time epoch of relative TFR was divided into time-frequency intervals to both test the effect of the movement on rhythmic activity modulation over time and assess differences due to the conditions (VALID_GO, INVALID_GO, INVALID_NO GO, and NEUTRAL). Specifically, mean relative power values were estimated by averaging relative TFR values in physiological bands and in the previously defined time intervals (pre_C, C1, C2, T1). According to Klimesch (1999), Individual Alpha Frequency (IAF) was obtained for each subject during the 3 min of rest with eyes closed and eyes open recorded at the beginning of the experimental session. The mean relative TFR values were then calculated in the following frequency bands: theta, from 4–Hz to IAF-3 Hz; low-alpha, from IAF-2 Hz to IAF; high-alpha, from IAF+1Hz to IAF+2 Hz; beta, from IAF +3 Hz–30 Hz.

2.6. Source analysis

To identify the neural sources underlining the differences in the modulation of rhythmic brain activity between conditions, we performed a current density analysis of the frequency domain in 3D MNI space using eLORETA (Pascual-Marqui, 2007) by means of LORETA software available at https://www.uzh.ch/keyinst/loreta.htm. First, the realistic electrode coordinates obtained by digitalization were fit onto the scalp template in MNI space by means of a 12-parameters affine transformation available in LORETA software. Then, the current source density distributions of each frequency band's power during the previously defined time intervals (pre_C, C1, C2, T1) and in pre-stimulus intervals were estimated by mean of eLORETA on a grid of 6239 voxels, with a spatial resolution of 5 mm for each subject and each condition. ERD/ERS were then evaluated for each voxel and cortical maps of the differences between conditions were calculated. Differences between conditions were visualized using an average cortex (Van Essen, 2005).

2.7. Statistical analysis

In terms of behavioural performance evaluation, time to reach the target level (TtM_2) was considered a dependent variable across the experimental conditions that included movements, i.e., the VALID_GO, INVALID_GO, and NEUTRAL conditions. A repeated measures ANOVA with a three levels within-subject factor was then performed (*Condition*). To exclude that possible differences among conditions depended on movement from high to low or low to high force levels, a control ANOVA design was applied on TtM_2, by adding a 4 levels within-subject factor (*Force Level*: 5%, 10%, 20%, 25% MVC) to the *Condition* factor.

To assess whether the level of force was stable before the target and ensure that the cue presentation did not distract the subject, potentially introducing a deviation from the required force level of 15% of MVC, FVi mean values across conditions in pre_C, C1, and C2 intervals were compared by a repeated measures ANOVA with a 3 levels within-subject factor (*Time*). Partial eta-squared (η_p^2) was used as a measure of effect size and post-hoc comparisons were performed by means of a paired *t*-test. To control for multiple comparison a Bonferroni correction was applied, adopting an alpha criterion of 0.05.

The main aim of the statistical analysis of the EEG data was to evaluate differences between the four conditions (VALID_GO, INVALID_GO, INVALID_NO GO, and NEUTRAL) in the T1 interval. For each frequency band, mean relative TFR values for the four experimental conditions in this interval were compared using a within-subject design by means of a non-parametric cluster-based test statistic with Monte Carlo randomization (Maris and Oostenveld, 2007), which takes the multiple comparison problem into account. Briefly, the four experimental conditions were compared at each EEG channel by means of an F value. All EEG channels showing an F value corresponding to a p value of less than 0.05 were selected and spatially distributed in clusters. The statistical cluster level was defined as the F sum in the channel belonging to the same cluster. The cluster with the maximal value was then utilized to build the statistics by randomizing the values in the different conditions 15,000 times. This statistics was then used to evaluate cluster significance at an alpha level of 0.05. Once significant clusters were found, post-hoc analysis was carried out by comparing pairs of conditions by means of paired t-tests. Additionally, a non-parametric clustering test with Monte Carlo randomization was applied with an alpha level of 0.025, corresponding to a false alarm rate of 0.05 in a two-sided test.

In the T1 interval, the latency of the ERD/ERS peaks of the averages of channels belonging to the significant clusters was evaluated for each subject and each condition. Repeated measures ANOVA was applied to latency values, with *Condition* (four levels: VALID_GO, INVALID_GO, INVALID_NO GO, and NEUTRAL) and *Cluster* as the within-subjects factors.

To assess differences between relative band power values in the cue period with respect to the pre_C interval, the mean TFR values across conditions (VALID_GO, INVALID_GO, and INVALID_NO GO) in both C1 and C2 intervals were compared to the values in the pre_C interval by means of paired sample *t*-test for each band. Non-parametric clustering test with Monte Carlo randomization was also applied. As control analysis, we also checked to make sure that no differences between the conditions were present prior to the target period.

3. Results

3.1. Behavioural results

Averaged values (±standard deviation) of TtM_1 (i.e., time needed to reach 15% of the MVC) across all the conditions were 1424 ± 342 ms. When the repeated measures ANOVA was applied to the FVi values (i.e., the force variation with respect to the required level of 15% MVC) with the three-level within-subject factor *Time* (pre_C, C1 and C2), a significant effect of *Time* was found [$F(1, 17) = 51.74$, $\eta^2 = 0.753$; $p < 0.0005$]. Post-hoc analysis indicated that the FVi value was higher in pre_C than in either the C1 or C2 intervals ($p < 0.001$ consistently) and that mean FVi values in the C1 interval were higher than those in the C2 interval ($p = 0.008$, Fig. 3, right panel), indicating a performance improvement.

TtM_2 values (i.e., the time needed to reach the target level in the T1 interval) for the three conditions (VALID_GO, INVALID_GO, and NEUTRAL) and their relative standard deviations were 938 ± 162 ms, 864 ± 120 ms, and 828 ± 164 ms, respectively. Repeated measures

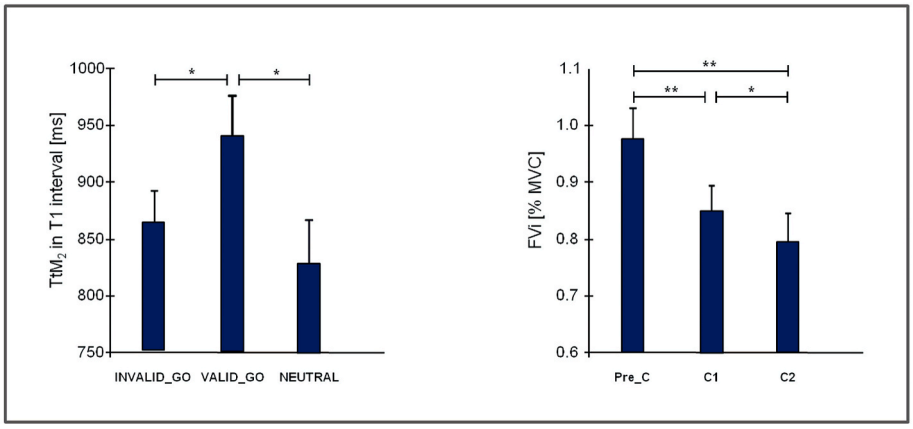

Fig. 3. On the left: mean (standard error) of Time to Movement in the target period (TtM2, i.e., the time required to reach the requested level) in INVALD_GO, VALID_GO, NEUTRAL conditions. On the right: mean (standard error) of the Force Variation index (FVi) in Pre_C, C1 and C2 intervals. Stars indicate significance of paired *t*-test (Bonferroni corrected): *p < 0.05, **p < 0.005.

ANOVA was applied to TtM_2 values with a single factor (*Condition*) design with the three levels (VALID_GO, INVALID_GO, and NEUTRAL); a significant effect of *Condition* [F (1, 34) = 7.38, $\eta^2 = 0.303$; p = 0.002] was found. Bonferroni-corrected post-hoc analysis indicated a significantly slower performance during VALID_GO with respect to INVALID_GO (corrected p = 0.015) and NEUTRAL (p = 0.011). No difference between INVALID_GO and NEUTRAL was observed (p > 0.20, Fig. 3, left panel). To exclude that these differences depended on the force level to be reached, an ANOVA design to TtM_2 values was applied, with *Condition* and *Force Level* as within-subject factors. The lack of interaction *Condition* x *Force Level* [F(3.9,65.6) = 1.00, p = 0.430; $\eta^2 = 0.056$] indicated that the observed differences between conditions was not dependent on force level. Indeed, for each level to be reached (5%, 10%, 20% and 25%) VALID_GO times were longer than the INVALID_GO and NEUTRAL times (p < 0.05, consistently).

3.2. EEG results

Fig. 1S (supplementary material) shows the overall average of the relative TFR across subjects. Eighteen locations are displayed, corresponding to the mean of the 10–20 system channels and their first neighbours and covering the fronto-polar (area around the Fp1, Fpz, and Fp2 electrodes of the 10–20 international system), frontal (F7, F3, Fz, F4, and F8), central (C3 and C4), temporal (T5 and T6), parietal (T7, P3, Pz, P4, and T8), and occipital (O1 and O2) areas. Visual inspection led to the defining of a large, sustained ERD in both the 8–15 Hz and 16–30 Hz bands (corresponding to the alpha and beta bands) during the movement in the posterior and centro-frontal areas, starting soon after stimulus onset, in each condition. A clear theta ERS was also present during the first second post-stimulus onset (i.e., trial onset), during the first second post-cue onset, and during the first second post-target onset.

To compare the cue interval time periods (C1 and C2) with the pre_C period, the relative TFR values of the INVALID_GO, VALID_GO,

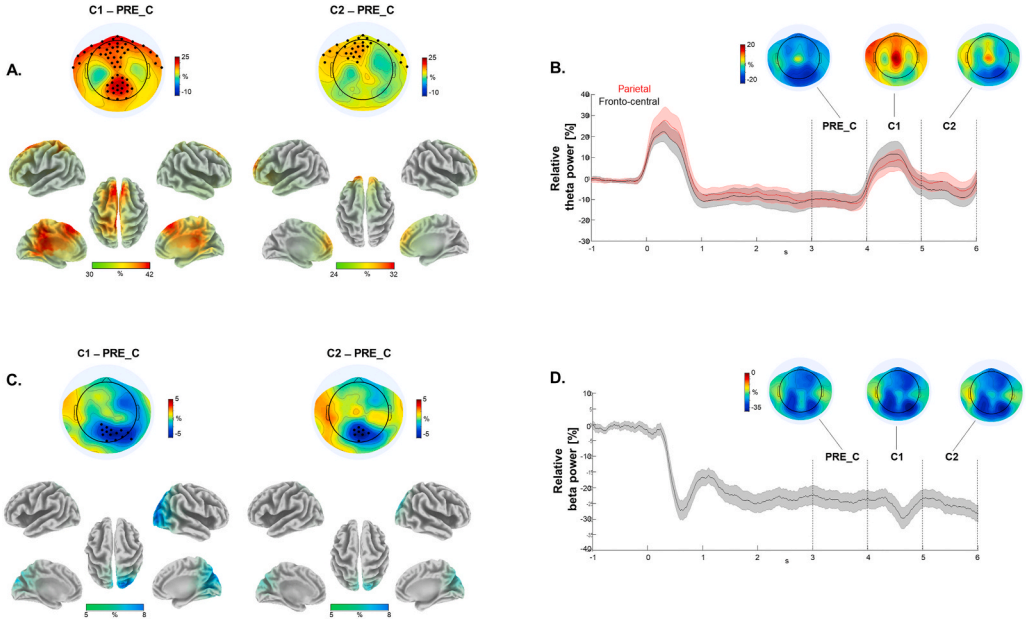

Fig. 4. A. Mean topography across subjects of the difference between theta ERS in C1 and in pre_C intervals and between theta ERS in C2 and pre_C intervals. Stars indicate significant clusters in the non-parametric comparison (C1 vs pre_C and C2 vs pre_C, respectively). The mean of C1 vs pre_C (and C2 vs pre_C) difference of theta ERS in the source space, obtained by eLORETA in frequency domain, is also shown. **B.** Mean across subjects (standard error is also shown) of the time course of theta modulation with respect to the pre-movement period (ERD/ERS) in the time window from 1 s before the trial onset (0 s) to the cue appearance (4 s) and the end of the cue period (6 s). The theta ERD/ERS activity of the EEG channels belonging to the significant clusters in the C1 interval displayed in A have been averaged (black: parietal, red: fronto-central). The Mean topographies across subjects of theta ERS in the pre_C, C1, C2 time intervals are shown. **C.and D.** The same as in A and B for beta frequency. . (For interpretation of the references to colour in this figure legend, the reader is referred to the Web version of this article.)

INVALID_NO GO conditions were averaged. As expected, no differences in relative TFR values were found across the INVALID_GO, VALID_GO, and INVALID_NO GO conditions in the pre_C, C1, and C2 intervals as per the non-parametric tests. Comparisons between the relative band powers of the pre_C and C1 intervals were carried out using non-parametric permutation tests. In the theta band, a fronto-central and a parietal cluster were found ($p < 0.001$ consistently) with a significant theta increase in these clusters in C1 with respect to pre_C interval. These clusters are shown in the topographic map of Fig. 4A (left panel) along with the C1 vs pre_C differences in theta ERS in the source space, which were obtained by eLORETA in frequency domain. These last maps indicate a higher theta immediately post-cue onset in the dorso-medial prefrontal cortex and the Posterior Parietal Cortex (PPC). In comparing the pre_C and C2 intervals, only a frontal cluster was found in the theta band ($p = 0.014$); it had a higher theta power in C2 as compared to the pre_C interval (Fig. 4A, right panel), which corresponded to increased theta activity in the dorso-medial prefrontal cortex. Additionally, no theta increase with respect to the pre_C period was found in the PPC; this is worth noting as it is a different result from that of the previous C1 interval. The mean values of the theta ERS in the frontal cluster were similar across the C2 and C1 intervals (paired *t*-test: $t(17) = -1.81$, $p = 0.09$). In the time evolution of theta ERS in the significant clusters, theta activity increased soon after the cue appearance and reduced after 1 s, more strongly in parietal regions (Fig. 4B).

In beta band, a cluster in posterior areas was found, indicating an increase in beta ERD in both the C1 ($p = 0.043$) and C2 ($p = 0.046$) intervals as compared to the pre_C interval (Fig. 4C). Differences in the beta ERD in the source space, as obtained by eLORETA in frequency domain, indicate lower beta activity in parieto-occipital regions (Fig. 4C). The beta ERD increased soon after cue onset and then not significantly decreased after 1 s (Fig. 4D).

A cluster-based non-parametric randomization test was applied to evidence differences between the VALID_GO, INVALID_GO, INVALID_NO GO, and NEUTRAL conditions in the T1 period. Two significant clusters were found in the theta band, one in the fronto-polar regions ($p = 0.047$) and one in the centro-parieto-occipital region ($p = 0.024$) (Fig. 5A). Post-hoc analysis (Fig. 5A and B) of the frontal cluster revealed that the theta ERS was higher in INVALID_GO than in either VALID_GO and INVALID_NO GO ($p = 0.001$ and $p = 0.015$, respectively). No differences were found between INVALID_GO and NEUTRAL or between VALID_GO and NEUTRAL conditions. Higher theta level was found in NEUTRAL than in INVALID_NO GO ($p = 0.030$). In the parieto-occipital regions, theta ERS in INVALID_GO and NEUTRAL conditions were higher than theta ERS in VALID and INVALID_NO GO ($p < 0.01$, consistently). No differences between VALID_GO and INVALID_NO GO were found. Fig. 5C shows the differences in theta ERS in INVALID_GO and NEUTRAL (pooled together) minus VALID_GO and INVALID_NO GO (pooled together) in the source space obtained by eLORETA in the frequency domain. These maps indicate a positive difference in the inmedial prefrontal and PPC/superior parietal cortices in theta.

Repeated measures ANOVA was applied to the latency of the theta ERS peak of the average of channels belonging to the significant frontal and parietal clusters. The within-subjects factors *Condition,* with four levels (VALID_GO, INVALID_GO, VALID_NOGO, and NEUTRAL), and

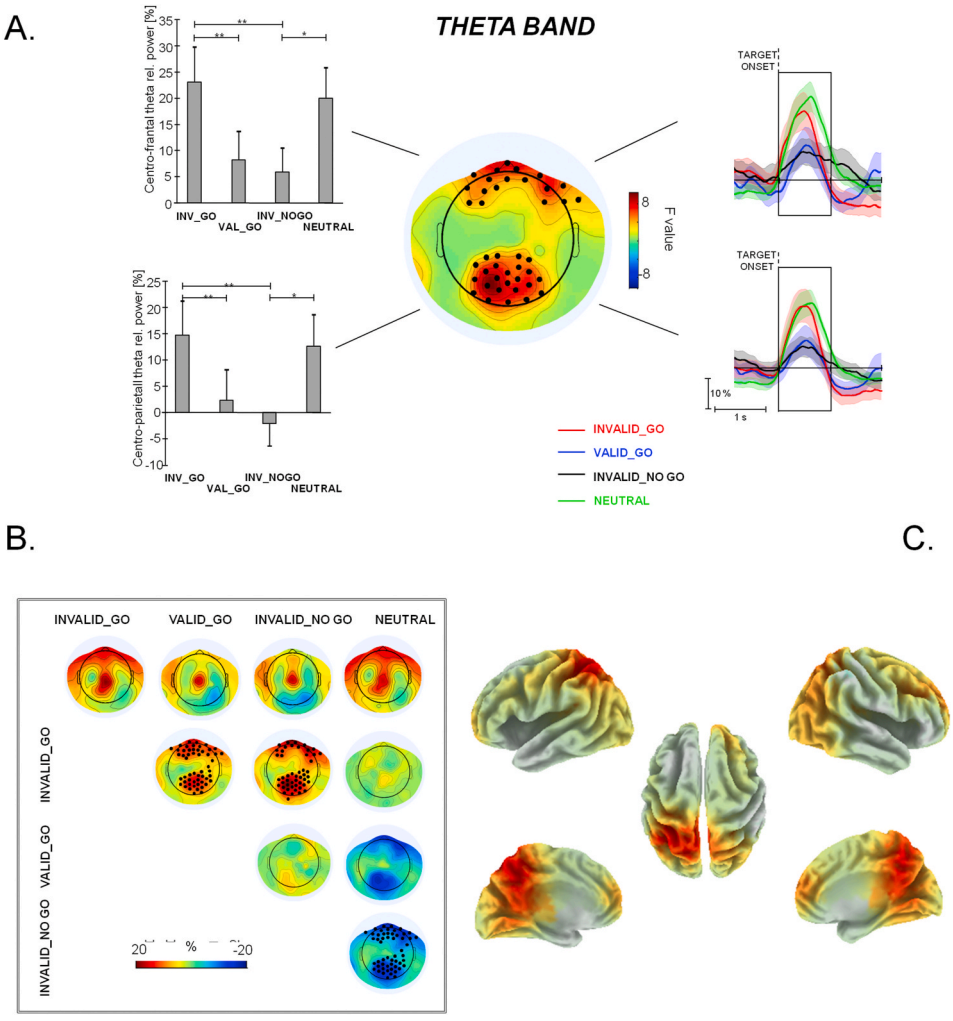

Fig. 5. A. Topography of F-values obtained by the within-subject comparison of conditions (INVALID_GO, VALID_GO, INVALID_NO GO, NEUTRAL) for theta ERS values in T1 interval. Stars indicate significant clusters in the non-parametric permutation test. Time courses of mean (standard error) across subjects of theta ERS values of EEG channels belonging to the prefrontal and parietal clusters are shown (INVALD_GO: red, VALID_GO: blue, INVALID_NO GO: black, NEUTRAL: green). On the left, the cluster mean values (standard errors) of theta ERS values are shown for each condition. Stars indicate significance of paired *t*-test (Bonferroni corrected) between conditions: *$p < 0.05$, **$p < 0.005$. **B**. First row: mean topographies across subjects of theta ERS in the experimental and NEUTRAL conditions. Differences between pair of conditions are shown in the second, third and fourth rows (specifically the difference between the condition indicated in the column on the right minus the condition indicated in the first row). Stars indicate significant clusters in the non-parametric permutation test performed to compare the two conditions. **C.** Difference of theta ERS in INVALID_GO and NEUTRAL (pooled together) minus VALID_GO and INVALID_NOGO (pooled together) in the source space obtained by eLORETA in frequency domain. . (For interpretation of the references to colour in this figure legend, the reader is referred to the Web version of this article.)

Cluster, with two (frontal and parietal) were considered. Only a significant effect of *Condition* [F (3, 51) = 5.66, $\eta^2 = 0.250$; p = 0.002] was found. Bonferroni-corrected post-hoc analysis indicated lower latency in INVALID_GO than in either VALID_GO (corrected p = 0.006, mean latency 310 ± 27 ms and 433 ± 46 ms, respectively) or INVALID_NO GO (p = 0.011, mean latency 486 ± 37 ms). No differences were observed between INVALID_GO and NEUTRAL (p = 0.154, mean latency of NEUTRAL theta ERS: 404 ± 37 ms), between VALID_GO and INVALID_NO GO, between VALID_GO and NEUTRAL, or between INVALID_NO GO and NEUTRAL (p > 0.200, consistently).

In the beta band, the cluster-based non-parametric randomization test was applied to the T1 period. A significant cluster was found in the left parieto-occipital areas (p = 0.044, Fig. 6A). Post-hoc analysis (Fig. 6A and B) revealed that the beta ERD was lower in NEUTRAL than in INVALID_GO, VALID, or INVALID_NO GO. Pair-wise comparisons, by means of a paired non-parametric clustering test, indicated that both INVALID_GO and VALID showed greater ERD than NEUTRAL in the beta band of the right fronto-polar electrodes (<0.025, consistently). Fig. 6C shows the differences of beta ERD in the experimental conditions (INVALID_GO, VALID_GO, and INVALID_NO GO pooled together) as compared to NEUTRAL in the source space obtained by eLORETA in the frequency domain. These maps indicate a higher beta ERD in the experimental conditions as compared to the control in occipital areas.

Repeated measures ANOVA was applied to the latency of the beta ERD peak of the average of channels in the significant cluster with the four level within-subjects factor *Condition* (VALID_GO, INVALID_GO, VALID_NO GO, and NEUTRAL). A significant effect of *Condition* [F(3, 51) = 13.71, $\eta^2 = 0.446$; p < 0.001] was found. Mean latency was 456 ± 83 ms for INVALID_GO condition, 717 ± 85 ms for VALID_GO, 573 ± 67 ms for INVALID_NO GO, and 680 ± 80 ms for NEUTRAL. Post-hoc analysis indicated significantly lower latency in INVALID_GO than in either VALID_GO (p = 0.001) or NEUTRAL (p = 0.001) while latency in VALID_GO was higher than in INVALID_NO GO (p = 0.015). No differences were observed between INVALID_GO and INVALID_NO GO (p = 0.122), between INVALID_NO GO and NEUTRAL (p = 0.085), or between VALID_GO and NEUTRAL (p > 0.200).

4. Discussion

Since Posner et al. first described the concept of IoR, many investigations have been conducted on this topic using different procedures (Amenedo et al., 2015; Klein, 2000; Spence et al., 2000). However, as far as we know, this is the first study designed to trace a sort of IoR time-lapse from cue appearance to response during a grip force control task. Indeed, the IoR temporal dynamics are usually studied by means of key press task, that is, through a procedure entailing an off-on transition from no motor action to a voluntary motor action. Although this way has been able to provide a remarkable amount of knowledge on IoR dynamics, it cannot disambiguate weather IoR effect observed on response times was due to slowed orienting of attention, slowed sensorial/perceptual processing and/or slowed initiation of the motor response. In this study we have applied a novel force-matching task, thus requiring to participants a "continuous" motor control (rather than an off-on action) during the entire cue-target period. Specifically, participants in this study watched a visual stimulus that displayed both the force level they were exerting and the force level they were asked to reach by varying their grip on the pneumatic device. Notably, participants exerted a steady level of force as they waited for the target to appear during the cue period, maintaining the cursor bar at the starting level. This force then had to be abruptly modified to reach the new target level. The described procedure was the same for all the experimental conditions. In addition to the advantage of obtaining a steady-state response rather than an off-on transition from no motor action to a voluntary motor action, this procedure allowed for an instant-by-instant

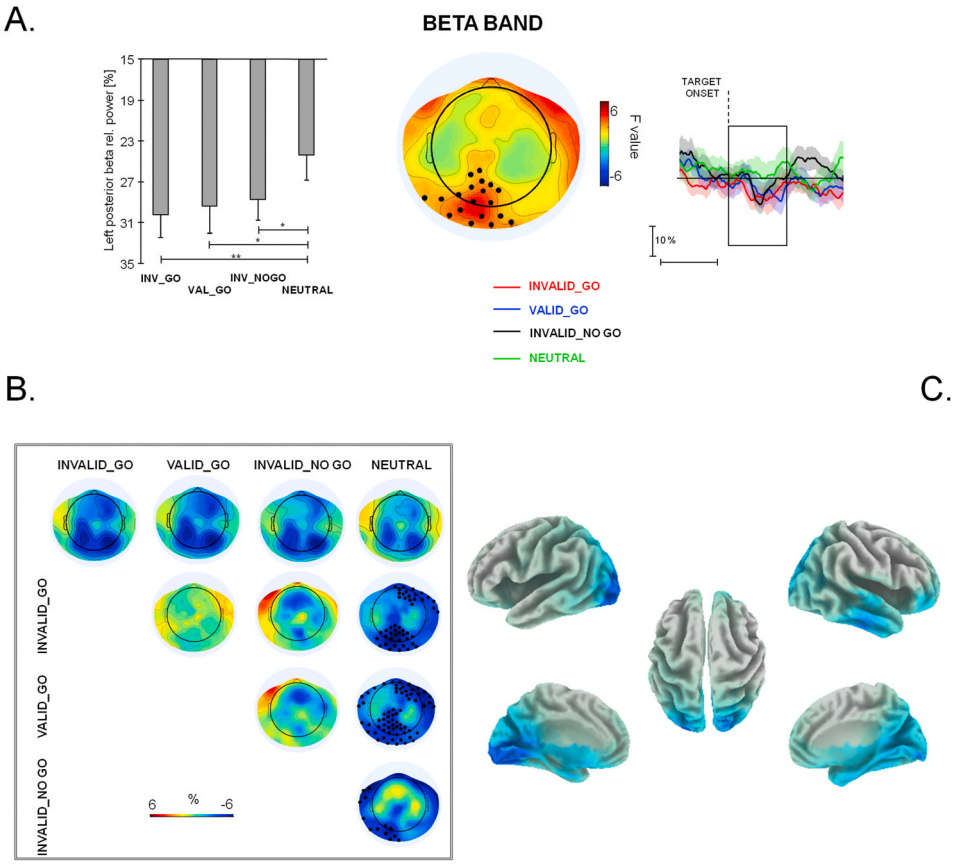

Fig. 6. A. Topography of F-values obtained by the within-subject comparison of conditions (INVALID_GO, VALID_GO, INVALID_NO GO, NEUTRAL) for beta ERD values in T1 interval. Stars indicate significant clusters in the non-parametric permutation test. Time courses of mean (standard error) across subjects of beta ERD values of EEG channels belonging to the posterior cluster is shown on the right (INVALID_GO: red, VALID_GO: blu, INVALID_NO GO: black, NEUTRAL: green). On the left, the cluster mean values (standard errors) of beta ERD values are shown. Stars indicate significance of paired *t*-test (Bonferroni corrected) between conditions: *p < 0.05, **p < 0.005. **B.** First row: mean topographies across subjects of beta ERD in the experimental and NEUTRAL conditions. Differences between pair of conditions are shown in the second, third and fourth rows (specifically the difference between the condition indicated in the column on the right minus the condition indicated in the first row). Stars indicate significant clusters in the non-parametric permutation test performed to compare the two conditions. **C.** Difference of beta ERD in experimental conditions (INVALID_GO, VALID_GO, INVALID_NO GO pooled together) vs NEUTRAL in the source space obtained by eLORETA in frequency domain. . (For interpretation of the references to colour in this figure legend, the reader is referred to the Web version of this article.)

observation of the entire time window from the start of the contraction through the cue appearance until the target level reached. Indeed, such an approach provides measurable behavioural correlations of the cue appearance effect, which are usually not available because a typical cue-target task does not require a motor response.

4.1. Cue interval

At the beginning of each trial, subjects were asked to reach and stably maintain a contraction level for 4 s. Comparison analysis of contraction stability between this period and the following cue interval showed that contraction stability increased with respect to the previous pre-cue time window after the cue's appearance. This evidence could be interpreted as an improvement in control capability due to the attention capture exerted by the cue. Indeed, it could also be suggested that, following the cue onset, the attention level increased when waiting for the target, thus improving the subject's readiness to respond thereto. This interpretation is supported by the oscillatory activity observed during the same time intervals (i.e., pre-cue and cue intervals). Indeed, in our study, oscillatory dynamics, as measured by comparing pre- and post-cue time intervals, showed significant theta ERS and beta ERD increases in fronto-central and parietal sites immediately post-cue onset followed by ERS and ERD decreases in the same frequency bands.

More precisely, a significant ERS in the fronto-central and parietal areas was observed during the first post-cue interval as compared to the pre-cue interval in theta band. This activity enhancement in the fronto-central regions could be explained using the "need of control" model created by Cavanagh and Frank (2004). Following them, during control operations in tasks involving unexpected situations, including, for example, conflicting response requirements, error detection, and novelty of stimuli, an increase in midline frontal activity in the theta band was observed. This activity, which is primarily generated in the anterior cingulate cortex (ACC) and the medial prefrontal cortex (supplementary motor area-SMA and preSMA), has been interpreted as a sort of 'lingua franca', that is, a trade language, a common mechanism for the adaptive control in a variety of context of uncertainty (Cavanagh et al., 2012; Cavanagh and Frank, 2004). Indeed, theta band modulation has often been observed in association with cognitive control tasks (Brunetti et al., 2019; Cooper et al., 2019; Li et al., 2015). Consequently, the frontal theta activity observed in our visual guided motor task could be considered to be an alarm clock for those mechanisms which require the integration of attention and sensorimotor processes, sensorimotor planning, intention of movement, error detection and correction, recruitment of executive control in interference situations, or conflict of monitoring systems (Mückschel et al., 2016; Pavone et al., 2016; Perfetti et al., 2011; Tombini et al., 2009). This alert status persisted along the entire cue period, as suggested by the significant increase in fronto-central theta ERS throughout the cue period until target appearance.

A parietal Theta ERS improvement, as compared to the pre-cue period, was also observed immediately post-cue appearance. Observed parietal involvement in a visuo-guided spatial task was not surprising; indeed, prominent neuroimaging and neuropsychological evidence has indicated a dual pathway model for perception, with a ventral "vision to perception" stream and a dorsal "action" pathway that interact (Gallivan and Goodale, 2018; Goodale and Milner, 1992; Mishkin et al., 1983; van Polanen and Davare, 2015). This dorsal way, which includes the posterior parietal cortex (PPC), is supposed to manage the transformation of received visual information into the performance of a motor action. Recent formulations also supposed a more complex involvement of human dorsal visual system in non-spatial information representation directed to visually-guided movements. Such representations could be useful in guiding the placement of the hand and fingers when an object manipulation is required. Following this model, PPC is considered as part of an integrated large-scale circuit supporting tool use and manipulation (see (Kastner et al., 2017) for a review). Consequently, the low-frequency modulation in this region post-cue onset could reflect the mechanism needed to generate environmental metrics and specific effectors for control of the hand force level. Interestingly, this mechanism, which acts as a facilitator after a short delay (i.e., a valid condition effect in a classic Posner task), reduced its engagement over time, as suggested by the observation of the following post-cue interval, in which a decreased parietal theta ERS was seen. This interpretation agrees with suggestions from Tian et al. (2011), who proposed a three-stage model in which post-cue ERP analysis was temporally divided into an early, a middle, and a late period, also known as a facilitation period, a transitional period, and a final behavioural inhibition period, respectively.

When examining beta band modulation in the same time windows, an increase of ERD in the right parieto-occipital areas was observed soon after cue appearance as compared to the pre-cue interval. To return to the frame of the dual pathways model of vision, this region of the dorsal stream is supposed to project to the posterior parietal cortex, thorough the superior colliculus, to generate a real world map and a motor plan (Gallivan and Goodale, 2018; Goodale and Milner, 1992). This result overlaps with the occipito-parietal cortex activation during the so called "late period" observed by Tian et al. (2011). In our data, activity in this area was enhanced post-cue onset and maintained a tonic response throughout the cue period.

To summarize, the observation of both theta and beta modulations during the cue period could lead one to argue that the steady-state response generated in the pre-cue period may have been abruptly interrupted by the cue's appearance, thus requiring a frontal "need of control" alarm along with increases of activity in parietal areas. This interpretation was supported by behavioural evidence of a variation in contraction, reinforcing the idea of attention capture by the cue. Finally, the parietal theta power increase lasted for about 1 s before returning to its pre-cue level. This behaviour could be interpreted as the neural correlate of the attention de-coupling evoked as the foundational mechanism of IoR (Posner and Cohen, 1984; Posner et al., 1985).

4.2. Target interval

After the cue period, the target appears, and the participant must modify her/his contraction force to reach the new location. Three circumstances can occur: i) the target location coincides with the cue location (VALID_GO); ii) the target location does not coincide with the cue location, meaning that a new location must be reached (INVALID_GO); iii) the target location does not coincide with the cue location such that the target appears at the starting position, meaning that action must be prevented while steady contraction must be maintained (INVALID_NO GO).

From a behavioural point of view, the time to reach the new level was measured across different conditions, revealing a significantly slower performance when the target location was the same as the cue. This result is consistent with previous evidence on the typical IoR effect, including the first observation by Posner et al. as well as more recent studies (Amenedo et al., 2015; Posner and Cohen, 1984; Prime and Ward, 2006). Indeed, a delayed response time was often observed when target stimuli appeared in the same cue location with a long cue-target time interval, suggesting an inhibitory after-effect to that stimuli (Klein, 2000). Notably, in our study, the time to response in the valid condition was also significantly slower as compared to in the neutral condition, that in which a target appeared without cue. This control condition was introduced to measure the individual response time to target regardless of where the target was expected to occur. It seems that the inhibitory mechanism provided a sort of negative tag (see Tian et al., 2011) on the cued position, and the cognitive cost of the attention reorienting toward this negatively tagged position was behaviourally translated in a response that slowed during the validly cued condition as compared to the control condition. Interestingly, no behavioural differences were observed between neutral control condition and the invalid one. One could speculate that, after a long cue-target time interval, the motor

control activated to produce a force contraction that is strong enough to reach the expected level (i.e., that suggested by the cue) is reset and a new force level has to be applied when the target appears in a new location that is different from what was expected; these circumstances were created by our neutral condition.

In examining oscillatory activity during this time window, frontal theta ERS was enhanced during INVALID_GO as compared to VALID_GO and INVALID_NO GO. Recent evidence suggests that frontal midline theta plays a key role in cognitive controls (Cavanagh and Frank, 2004; Nigbur et al., 2011). Specifically, the involvement of the theta rhythm in a wide span of cognitive processes, including focused attention, novelty encoding, working memory loading, and top-down cognitive control, has been recognized (Brunetti et al., 2019; Cavanagh and Frank, 2004; Fiebelkorn and Kastner, 2019). One could argue that the observed frontal theta amplitude enhancement after target onset in a new, unattended position (i.e., INVALID_GO) represented the top-down cognitive load needed to promptly encode and respond to the target. In a recent paper, Pellegrino et al. tested differences in theta oscillation during motor reprogramming versus motor re-evaluation. Following them, theta activity in the fronto-central cortical regions significantly increased when the pre-cue was invalid and required subjects to select an alternate response. They concluded that frontal theta is functionally relevant when unattended after-cue action was required; essentially, when a re-adjustment of cue-induced action was needed (Pellegrino et al., 2018). Moreover, to explain the reduced frontal theta in the VALID_GO and INVALID_NO GO conditions, we hypothesize that an inhibitory mechanism operates, though differently: inhibition to process the target in the cued location and inhibition of the motor response, respectively. It could be speculated that, during both VALID_GO and INVALID_NO GO conditions, the readiness demand was reduced, as compared to the INVALID_GO condition, due to the inhibition processes, which affected each condition differently. The model proposed by Prime and Ward (2006, 2004) could be considered an interpretative reference in this regard, as they hypothesized that IoR occurs due to a reduction in the salience of the cued location, thus reducing efficacy in terms of the processing of the target (Prime and Ward, 2006). The theta reduction during the VALID_GO condition, as observed in our results, could represent the neural correlate of salience reduction for validly cued targets. These interpretations were both supported by our latency results; theta ERS peak latency was delayed in both VALID_GO and INVALID_NOGO when compared to INVALID_GO, suggesting that the described inhibitory mechanisms could slow the response in these regions.

In terms of parieto-occipital theta band oscillation, ERS amplitude was enhanced during the INVALID_GO and NEUTRAL conditions as compared to VALID_GO and INVALID_NO GO. INVALID_GO and NEUTRAL should share a characteristic; in both conditions, the cue's effect on target response may be absent due to either a long cue-target interval (INVALID_GO) or to lack of a cue (NEUTRAL). Consequently, we could argue that what we observed in these conditions was the neural correlate of the orientation process toward novel and unattended stimuli, which is typically observed in visuo-spatial attention tasks. Previous studies demonstrated the role of the posterior superior parietal lobule in the preparation and redirection of movements and movement intentions (Gallivan and Goodale, 2018; Pellegrino et al., 2018) in complex behaviours like eye-hand coordination (see (Hadjidimitrakis et al., 2019) for a review), tactile shape recognition (Savini et al., 2010) (Savini et al., 2010), position and force signals integration for perception of stiffness (Leib et al., 2016) and, in general, its crucial role in spatial cognition (Szczepanski et al., 2010). We could argue that this region was also involved in our task, in which a force adjustment rather than a movement initiation was required. The increased theta ERS observed in the occipital areas could reflect an early target encoding, and the latency delay shown in VALID_GO and INVALID_NO GO (i.e., in those conditions in which inhibition was supposed to be active) could represent the additional time cost required to activate a previously inhibited stimulus or inhibit a previously activated stimulus, respectively.

A different behaviour was observed in the beta band. Indeed, when the target occurred, parieto-occipital beta ERD increased in the three cued conditions as compared to the neutral one. This result suggests an activity enhancement in parieto-occipital areas in those conditions in which a cue had been presented before the target. These three conditions are supposed to induce target location expectancy as compared to the neutral ones where a target was presented without location attendance. Consequently, in these three conditions, the target onset was preceded by a period in which motor planning based on the cue location was supposed to be prepared. When the target appeared, the previously planned contraction level had to be varied due to: i) an unexpected target location (INVALID_GO); ii) motor inhibition (INVALID_NO GO) or iii) activation of a previously inhibited location (VALID_GO). The engagement of the parieto-occipital regions in mechanisms of guiding actions that are putatively activated when a new, unexpected location must be reached has been previously suggested (Gallivan and Goodale, 2018). Additionally, beta is involved in the maintenance of the status-quo and is therefore reduced (i.e., ERD is enhanced) by attention shifts, i.e., when the status quo is interrupted (Engel and Fries, 2010; Richter et al., 2019). Interestingly, our data suggests that the activity oriented to respond to an unexpected location increased in all three experimental conditions, including the VALID_GO condition, namely when the correct location was indicated by the cue. This pattern could suggest that the long cue-target interval resets the planned force level to react according to visual feedback. Finally, data from the latency of beta ERD suggests that activity in these regions was faster during the INVALID_GO condition than the VALID_GO or NEUTRAL, that is, during attentional reorienting without inhibition.

To summarize, after the target onset, an articulate pattern of oscillatory activity was observed. A widespread fronto-parietal activity increase in the theta band occurred when the target appeared in an unexpected location, indicating a general alarm activation and an orientation toward a new, unexplored location by those regions involved in the so-called dorsal-action pathway. Moreover, the same frequency band showed reduced activity and delayed latency in those conditions in which an inhibitory process was supposed to act (i.e., inhibition of return or inhibition of movement). Such delayed activity could be interpreted as the neural correlate of the time cost that was observed behaviourally during IoR trials. Finally, a more posterior beta band modulation was observed when the target was preceded by a cue in those regions involved in guiding action mechanisms, suggesting a sort of "status quo" interruption and a motor program reset.

4.3. Conclusion

To conclude, the evidence presented in this study offers some insight into the ongoing debate regarding the processing stage in which mechanism underlying IoR acts: attentional/pre-motor or motor. Starting from the observation of oscillatory activity post-cue appearance, our results suggest a prominent involvement of the fronto-parietal and occipital cortical areas with a peculiar theta band modulation that characterizes the posterior parietal cortex. Specifically, the activity in this region, previously defined as a core region of the dorsal action pathway, was enhanced in response to the cue, decreased over time, and then was enhanced again when a target appeared in an unexpected location rather than the cued position. This evidence indicates an early complex mechanism that could act post-cue appearance to prepare a contraction level that is appropriate for reaching all locations except the cued one. This conclusion was supported by the observed involvement of the posterior parietal cortex, which is supposed to generate world metrics to help humans interact with the spatial environment. The oscillatory activity observed here indicates a sort of disinvestment from a recently explored spatial location, thus abolishing the relative motor plan. Therefore, we suggest that the inhibitory mechanism at the basis of IoR sequentially affects both perceptual/attentional processing and motor

preparation as opposed to response execution.

Appendix A. Supplementary data

Supplementary data to this article can be found online at https://doi.org/10.1016/j.neuropsychologia.2021.108068.

Credit author statement

Filippo Zappasodi: Conceptualization; Methodology; Investigation; Formal analysis; Investigation; Project administration. Pierpaolo Croce: Software; Formal analysis; Investigation; Data curation; Funding acquisition. Rosalia Di Matteo: Writing – review & editing; Supervision; Funding acquisition. Marcella Brunetti: Writing; Conceptualization; Methodology; Supervision; Funding acquisition; Project administration.

Author notes

This work was partially supported by the 'Department of Excellence 2018–2022' initiative of the Italian Ministry of Education, University and Research for the Department of Neuroscience, Imaging and Clinical Sciences (DNISC) of the University of Chieti-Pescara and by the 'Search of Excellence', initiative of the Department of Neuroscience, Imaging and Clinical Sciences (DNISC) of the University of Chieti-Pescara. Authors thank Carlo Cottone and Franca Tecchio for technical contribution and assistance. The authors report no personal or financial conflicts of interest related to the research reported herein.

References

Amenedo, E., Gutiérrez-Domínguez, F.-J., Darriba, Á., Pazo-Álvarez, P., 2015. Spatial Inhibition of Return promotes changes in response-related mu and beta oscillatory patterns. Neuroscience 310, 616–628. https://doi.org/10.1016/j.neuroscience.2015.09.072.

Barbati, G., Porcaro, C., Zappasodi, F., Rossini, P.M., Tecchio, F., 2004. Optimization of an independent component analysis approach for artifact identification and removal in magnetoencephalographic signals. Clin. Neurophysiol. Off. J. Int. Fed. Clin. Neurophysiol. 115, 1220–1232. https://doi.org/10.1016/j.clinph.2003.12.015.

Benchenane, K., Tiesinga, P.H., Battaglia, F.P., 2011. Oscillations in the prefrontal cortex: a gateway to memory and attention. Curr. Opin. Neurobiol., Behavioural and cognitive neuroscience 21, 475–485. https://doi.org/10.1016/j.conb.2011.01.004.

Berlucchi, G., 2006. Inhibition of return: a phenomenon in search of a mechanism and a better name. Cogn. Neuropsychol. 23, 1065–1074. https://doi.org/10.1080/02643290600588426.

Brunetti, M., Zappasodi, F., Croce, P., Di Matteo, R., 2019. Parsing the Flanker task to reveal behavioral and oscillatory correlates of unattended conflict interference. Sci. Rep. 9, 1–11. https://doi.org/10.1038/s41598-019-50464-x.

Brunetti, M., Zappasodi, F., Marzetti, L., Perrucci, M.G., Cirillo, S., Romani, G.L., Pizzella, V., Aureli, T., 2014. Do you know what I mean? Brain oscillations and the understanding of communicative intentions. Front. Hum. Neurosci. 8 https://doi.org/10.3389/fnhum.2014.00036.

Cavanagh, J.F., Frank, M.J., 2004. Frontal theta as a mechanism for cognitive control. Trends Cognit. Sci. 18, 414–421. https://doi.org/10.1016/j.tics.2014.04.012.

Cavanagh, J.F., Zambrano-Vazquez, L., Allen, J.J.B., 2012. Theta lingua franca: a common mid-frontal substrate for action monitoring processes. Psychophysiology 49, 220–238. https://doi.org/10.1111/j.1469-8986.2011.01293.x.

Chica, A.B., Taylor, T.L., Lupiáñez, J., Klein, R.M., 2010. Two mechanisms underlying inhibition of return. Exp. Brain Res. 201, 25–35. https://doi.org/10.1007/s00221-009-2004-1.

Classen, J., Gerloff, C., Honda, M., Hallett, M., 1998. Integrative visuomotor behavior is associated with interregionally coherent oscillations in the human brain. J. Neurophysiol. 79, 1567–1573. https://doi.org/10.1152/jn.1998.79.3.1567.

Clayton, M.S., Yeung, N., Kadosh, R.C., 2015. The roles of cortical oscillations in sustained attention. Trends Cognit. Sci. 19, 188–195. https://doi.org/10.1016/j.tics.2015.02.004.

Cooper, P.S., Karayanidis, F., McKewen, M., McLellan-Hall, S., Wong, A.S.W., Skippen, P., Cavanagh, J.F., 2019. Frontal theta predicts specific cognitive control-induced behavioural changes beyond general reaction time slowing. Neuroimage 189, 130–140. https://doi.org/10.1016/j.neuroimage.2019.01.022.

Croce, P., Zappasodi, F., Marzetti, L., Merla, A., Pizzella, V., Chiarelli, A.M., 2019. Deep convolutional neural networks for feature-less automatic classification of independent components in multi-channel electrophysiological brain recordings. IEEE Trans. Biomed. Eng. 66, 2372–2380. https://doi.org/10.1109/TBME.2018.2889512.

Davare, M., Andres, M., Clerget, E., Thonnard, J.-L., Olivier, E., 2007. Temporal dissociation between hand shaping and grip force scaling in the anterior intraparietal area. J. Neurosci. Off. J. Soc. Neurosci. 27, 3974–3980. https://doi.org/10.1523/JNEUROSCI.0426-07.2007.

Engel, A.K., Fries, P., 2010. Beta-band oscillations–signalling the status quo? Curr. Opin. Neurobiol. 20, 156–165. https://doi.org/10.1016/j.conb.2010.02.015.

Fiebelkorn, I.C., Kastner, S., 2019. A rhythmic theory of attention. Trends Cognit. Sci. 23, 87–101. https://doi.org/10.1016/j.tics.2018.11.009.

Gallivan, J.P., Goodale, M.A., 2018. Chapter 23 - the dorsal "action" pathway. In: Vallar, G., Coslett, H.B. (Eds.), Handbook of Clinical Neurology, the Parietal Lobe. Elsevier, pp. 449–466. https://doi.org/10.1016/B978-0-444-63622-5.00023-1.

Goodale, M.A., Milner, A.D., 1992. Separate visual pathways for perception and action. Trends Neurosci. 15, 20–25. https://doi.org/10.1016/0166-2236(92)90344-8.

Hadjidimitrakis, K., Bakola, S., Wong, Y.T., Hagan, M.A., 2019. Mixed spatial and movement representations in the primate posterior parietal cortex. Front. Neural Circ. 13, 15. https://doi.org/10.3389/fncir.2019.00015.

Kastner, S., Chen, Q., Jeong, S.K., Mruczek, R.E.B., 2017. A brief comparative review of primate posterior parietal cortex: a novel hypothesis on the human toolmaker. Neuropsychologia 105, 123–134. https://doi.org/10.1016/j.neuropsychologia.2017.01.034.

Klein, null, 2000. Inhibition of return. Trends Cognit. Sci. 4, 138–147. https://doi.org/10.1016/s1364-6613(00)01452-2.

Klein, R.M., Taylor, T.L., 1994. Categories of cognitive inhibition with reference to attention. In: Inhibitory Processes in Attention, Memory, and Language. Academic Press, San Diego, CA, US, pp. 113–150.

Klimesch, W., 1999. EEG alpha and theta oscillations reflect cognitive and memory performance: a review and analysis. Brain Res. Rev. 29, 169–195. https://doi.org/10.1016/S0165-0173(98)00056-3.

Kuhtz-Buschbeck, J.P., Ehrsson, H.H., Forssberg, H., 2001. Human brain activity in the control of fine static precision grip forces: an fMRI study. Eur. J. Neurosci. 14, 382–390. https://doi.org/10.1046/j.0953-816x.2001.01639.x.

Leib, R., Mawase, F., Karniel, A., Donchin, O., Rothwell, J., Nisky, I., Davare, M., 2016. Stimulation of PPC affects the mapping between motion and force signals for stiffness perception but not motion control. J. Neurosci. Off. J. Soc. Neurosci. 36, 10545–10559. https://doi.org/10.1523/JNEUROSCI.1178-16.2016.

Li, Q., Wang, K., Nan, W., Zheng, Y., Wu, H., Wang, H., Liu, X., 2015. Electrophysiological dynamics reveal distinct processing of stimulus-stimulus and stimulus-response conflicts: distinct processing of S-S and S-R conflicts. Psychophysiology 52, 562–571. https://doi.org/10.1111/psyp.12382.

Liebe, S., Hoerzer, G.M., Logothetis, N.K., Rainer, G., 2012. Theta coupling between V4 and prefrontal cortex predicts visual short-term memory performance. Nat. Neurosci. 15 (456–462), S1–S2. https://doi.org/10.1038/nn.3038.

Maris, E., Oostenveld, R., 2007. Nonparametric statistical testing of EEG- and MEG-data. J. Neurosci. Methods 164, 177–190. https://doi.org/10.1016/j.jneumeth.2007.03.024.

McDonald, J.J., Hickey, C., Green, J.J., Whitman, J.C., 2009. Inhibition of return in the covert deployment of attention: evidence from human electrophysiology. J. Cognit. Neurosci. 21, 725–733. https://doi.org/10.1162/jocn.2009.21042.

McDonald, J.J., Ward, L.M., 1999. Spatial relevance determines facilitatory and inhibitory effects of auditory covert spatial orienting. J. Exp. Psychol. Hum. Percept. Perform. 25, 1234–1252. https://doi.org/10.1037/0096-1523.25.5.1234.

Mishkin, M., Ungerleider, L.G., Macko, K.A., 1983. Object vision and spatial vision: two cortical pathways. Trends Neurosci. 6, 414–417. https://doi.org/10.1016/0166-2236(83)90190-X.

Mitra, P.P., Pesaran, B., 1999. Analysis of dynamic brain imaging data. Biophys. J. 76, 691–708. https://doi.org/10.1016/S0006-3495(99)77236-X.

Mückschel, M., Stock, A.-K., Dippel, G., Chmielewski, W., Beste, C., 2016. Interacting sources of interference during sensorimotor integration processes. Neuroimage 125, 342–349. https://doi.org/10.1016/j.neuroimage.2015.09.075.

Neuper, C., Pfurtscheller, G., 2001. Event-related dynamics of cortical rhythms: frequency-specific features and functional correlates. Int. J. Psychophysiol. Off. J. Int. Organ. Psychophysiol. 43, 41–58. https://doi.org/10.1016/s0167-8760(01)00178-7.

Nigbur, R., Ivanova, G., Stürmer, B., 2011. Theta power as a marker for cognitive interference. Clin. Neurophysiol. 122, 2185–2194. https://doi.org/10.1016/j.clinph.2011.03.030.

Oldfield, R.C., 1971. The assessment and analysis of handedness: the Edinburgh inventory. Neuropsychologia 9, 97–113.

Oostenveld, R., Fries, P., Maris, E., Schoffelen, J.-M., 2011. FieldTrip: open source software for advanced analysis of MEG, EEG, and invasive electrophysiological data. Comput. Intell. Neurosci. 156869. https://doi.org/10.1155/2011/156869, 2011.

Papadelis, C., Arfeller, C., Erla, S., Nollo, G., Cattaneo, L., Braun, C., 2016. Inferior frontal gyrus links visual and motor cortices during a visuomotor precision grip force task. Brain Res. 1650, 252–266. https://doi.org/10.1016/j.brainres.2016.09.011.

Pascual-Marqui, R.D., 2007. Discrete, 3D Distributed, Linear Imaging Methods of Electric Neuronal Activity. Part 1: Exact, Zero Error Localization. ArXiv07103341 Math-Ph Physicsphysics Q-Bio.

Pastötter, B., Hanslmayr, S., Bäuml, K.-H., 2008. Inhibition of return arises from inhibition of response processes: an analysis of oscillatory beta activity. J. Cognit. Neurosci. 20, 65–75. https://doi.org/10.1162/jocn.2008.20010.

Pavone, E.F., Tieri, G., Rizza, G., Tidoni, E., Grisoni, L., Aglioti, S.M., 2016. Embodying others in immersive virtual reality: electro-cortical signatures of monitoring the errors in the actions of an avatar seen from a first-person perspective. J. Neurosci. 36, 268–279. https://doi.org/10.1523/JNEUROSCI.0494-15.2016.

Pellegrino, G., Tomasevic, L., Herz, D.M., Larsen, K.M., Siebner, H.R., 2018. Theta activity in the left dorsal premotor cortex during action Re-evaluation and motor reprogramming. Front. Hum. Neurosci. 12 https://doi.org/10.3389/fnhum.2018.00364.

Perfetti, B., Moisello, C., Landsness, E.C., Kvint, S., Pruski, A., Onofrj, M., Tononi, G., Ghilardi, M.F., 2011. Temporal evolution of oscillatory activity predicts performance in a choice-reaction time reaching task. J. Neurophysiol. 105, 18–27. https://doi.org/10.1152/jn.00778.2010.

Pfurtscheller, G., Lopes da Silva, F.H., 1999. Event-related EEG/MEG synchronization and desynchronization: basic principles. Clin. Neurophysiol. Off. J. Int. Fed. Clin. Neurophysiol. 110, 1842–1857.

Pfurtscheller, G., Stancák, A., Neuper, C., 1996a. Event-related synchronization (ERS) in the alpha band–an electrophysiological correlate of cortical idling: a review. Int. J. Psychophysiol. Off. J. Int. Organ. Psychophysiol. 24, 39–46. https://doi.org/10.1016/s0167-8760(96)00066-9.

Pfurtscheller, G., Stancák, A., Neuper, C., 1996b. Post-movement beta synchronization. A correlate of an idling motor area? Electroencephalogr. Clin. Neurophysiol. 98, 281–293. https://doi.org/10.1016/0013-4694(95)00258-8.

Posner, M., Cohen, Y., 1984. Components of visual orienting. Atten. Perform. X control lang. Process 32, 531.

Posner, M.I., Rafal, R.D., Choate, L.S., Vaughan, J., 1985. Inhibition of return: neural basis and function. Cogn. Neuropsychol. 2, 211–228. https://doi.org/10.1080/02643298508252866.

Prime, D.J., Ward, L.M., 2006. Cortical expressions of inhibition of return. Brain Res. 1072, 161–174. https://doi.org/10.1016/j.brainres.2005.11.081.

Prime, D.J., Ward, L.M., 2004. Inhibition of return from stimulus to response. Psychol. Sci. 15, 272–276. https://doi.org/10.1111/j.0956-7976.2004.00665.x.

Rafal, R.D., Calabresi, P.A., Brennan, C.W., Sciolto, T.K., 1989. Saccade preparation inhibits reorienting to recently attended locations. J. Exp. Psychol. Hum. Percept. Perform. 15, 673–685. https://doi.org/10.1037//0096-1523.15.4.673.

Richter, C.G., Bosman, C.A., Vezoli, J., Schoffelen, J.-M., Fries, P., 2019. Brain Rhythms Shift and Deploy Attention. https://doi.org/10.1101/795567 bioRxiv 795567.

Samuel, A.G., Kat, D., 2003. Inhibition of return: a graphical meta-analysis of its time course and an empirical test of its temporal and spatial properties. Psychon. Bull. Rev. 10, 897–906. https://doi.org/10.3758/bf03196550.

Sauseng, P., Griesmayr, B., Freunberger, R., Klimesch, W., 2010. Control mechanisms in working memory: a possible function of EEG theta oscillations. Neurosci. Biobehav. Rev., Binding Processes: Neurodynamics and Functional Role in Memory and Action 34, 1015–1022. https://doi.org/10.1016/j.neubiorev.2009.12.006.

Savini, N., Babiloni, C., Brunetti, M., Caulo, M., Del Gratta, C., Perrucci, M.G., Rossini, P. M., Romani, G.L., Ferretti, A., 2010. Passive tactile recognition of geometrical shape in humans: an fMRI study. Brain Res. Bull. 83, 223–231. https://doi.org/10.1016/j.brainresbull.2010.08.001.

Schnitzler, A., Gross, J., 2005. Normal and pathological oscillatory communication in the brain. Nat. Rev. Neurosci. 6, 285–296. https://doi.org/10.1038/nrn1650.

Spence, C., Lloyd, D., McGlone, F., Nicholls, M.E.R., Driver, J., 2000. Inhibition of return is supramodal: a demonstration between all possible pairings of vision, touch, and audition. Exp. Brain Res. 134, 42–48. https://doi.org/10.1007/s002210000442.

Szczepanski, S.M., Konen, C.S., Kastner, S., 2010. Mechanisms of spatial attention control in frontal and parietal cortex. J. Neurosci. 30, 148–160. https://doi.org/10.1523/JNEUROSCI.3862-09.2010.

Tian, Y., Klein, R.M., Satel, J., Xu, P., Yao, D., 2011. Electrophysiological explorations of the cause and effect of inhibition of return in a cue-target paradigm. Brain Topogr. 24, 164–182. https://doi.org/10.1007/s10548-011-0172-3.

Tombini, M., Zappasodi, F., Zollo, L., Pellegrino, G., Cavallo, G., Tecchio, F., Guglielmelli, E., Rossini, P.M., 2009. Brain activity preceding a 2D manual catching task. Neuroimage 47, 1735–1746. https://doi.org/10.1016/j.neuroimage.2009.04.046.

Van Essen, D.C., 2005. A Population-Average, Landmark- and Surface-based (PALS) atlas of human cerebral cortex. Neuroimage 28, 635–662. https://doi.org/10.1016/j.neuroimage.2005.06.058.

van Polanen, V., Davare, M., 2015. Interactions between dorsal and ventral streams for controlling skilled grasp. Neuropsychologia 79, 186–191. https://doi.org/10.1016/j.neuropsychologia.2015.07.010.

von Stein, A., Chiang, C., König, P., 2000. Top-down processing mediated by interareal synchronization. Proc. Natl. Acad. Sci. U. S. A. 97, 14748–14753.

Zaepffel, M., Brochier, T., 2012. Planning of visually guided reach-to-grasp movements: inference from reaction time and contingent negative variation (CNV). Psychophysiology 49, 17–30. https://doi.org/10.1111/j.1469-8986.2011.01277.x.